



**HAL**  
open science

## Experience with wavefront sensor and deformable mirror interfaces for wide-field adaptive optics systems

A G Basden, D. Atkinson, N A Bharmal, U. Bitenc, M. Brangier, T. Buey, T. Butterley, D. Cano, Fanny Chemla, P. Clark, et al.

### ► To cite this version:

A G Basden, D. Atkinson, N A Bharmal, U. Bitenc, M. Brangier, et al.. Experience with wavefront sensor and deformable mirror interfaces for wide-field adaptive optics systems. Monthly Notices of the Royal Astronomical Society, 2016, 459 (2), pp.1350-1359. 10.1093/mnras/stw730 . hal-04511252v2

**HAL Id: hal-04511252**

**<https://hal.science/hal-04511252v2>**

Submitted on 19 Mar 2024

**HAL** is a multi-disciplinary open access archive for the deposit and dissemination of scientific research documents, whether they are published or not. The documents may come from teaching and research institutions in France or abroad, or from public or private research centers.

L'archive ouverte pluridisciplinaire **HAL**, est destinée au dépôt et à la diffusion de documents scientifiques de niveau recherche, publiés ou non, émanant des établissements d'enseignement et de recherche français ou étrangers, des laboratoires publics ou privés.

## Durham Research Online

---

### Deposited in DRO:

06 May 2016

### Version of attached file:

Published Version

### Peer-review status of attached file:

Peer-reviewed

### Citation for published item:

Basden, A. G. and Atkinson, D. and Bharmal, N. A. and Bitenc, U. and Brangier, M. and Buey, T. and Butterley, T. and Cano, D. and Chemla, F. and Clark, P. and Cohen, M. and Conan, J.-M. and de Cos, F. J. and Dickson, C. and Dipper, N. A. and Dunlop, C. N. and Feautrier, P. and Fusco, T. and Gach, J. L. and Gendron, E. and Geng, D. and Goodsell, S. J. and Gratadour, D. and Greenaway, A. H. and Guesalaga, A. and Guzman, C. D. and Henry, D. and Holck, D. and Hubert, Z. and Huet, J. M. and Kellerer, A. and Kulcsar, C. and Laporte, P. and Le Roux, B. and Looker, N. and Longmore, A. J. and Marteau, M. and Martin, O. and Meimon, S. and Morel, C. and Morris, T. J. and Myers, R. M. and Osborn, J. and Perret, D. and Petit, C. and Raynaud, H. and Reeves, A. P. and Rousset, G. and Sanchez Lasheras, F. and Sanchez Rodriguez, M. and Santos, J. D. and Sevin, A. and Sivo, G. and Stadler, E. and Stobie, B. and Talbot, G. and Todd, S. and Vidal, F. and Younger, E. J. (2016) 'Experience with wavefront sensor and deformable mirror interfaces for wide-field adaptive optics systems.', *Monthly notices of the Royal Astronomical Society.*, 459 (2). pp. 1350-1359.

### Further information on publisher's website:

<http://dx.doi.org/10.1093/mnras/stw730>

### Publisher's copyright statement:

This article has been accepted for publication in *Monthly notices of the Royal Astronomical Society* ©: 2016 The Authors Published by Oxford University Press on behalf of the Royal Astronomical Society. All rights reserved.

### Additional information:

### Use policy

---

The full-text may be used and/or reproduced, and given to third parties in any format or medium, without prior permission or charge, for personal research or study, educational, or not-for-profit purposes provided that:

- a full bibliographic reference is made to the original source
- a [link](#) is made to the metadata record in DRO
- the full-text is not changed in any way

The full-text must not be sold in any format or medium without the formal permission of the copyright holders.

Please consult the [full DRO policy](#) for further details.

# Experience with wavefront sensor and deformable mirror interfaces for wide-field adaptive optics systems

A. G. Basden,<sup>1\*</sup> D. Atkinson,<sup>2</sup> N. A. Bharmal,<sup>1</sup> U. Bitenc,<sup>1</sup> M. Brangier,<sup>3</sup> T. Buey,<sup>3</sup> T. Butterley,<sup>1</sup> D. Cano,<sup>4</sup> F. Chemla,<sup>5</sup> P. Clark,<sup>1</sup> M. Cohen,<sup>5</sup> J.-M. Conan,<sup>6</sup> F. J. de Cos,<sup>7</sup> C. Dickson,<sup>2</sup> N. A. Dipper,<sup>1</sup> C. N. Dunlop,<sup>1</sup> P. Feautrier,<sup>8</sup> T. Fusco,<sup>6,9</sup> J. L. Gach,<sup>9</sup> E. Gendron,<sup>3</sup> D. Geng,<sup>1</sup> S. J. Goodsell,<sup>1</sup> D. Gratadour,<sup>3</sup> A. H. Greenaway,<sup>10</sup> A. Guesalaga,<sup>11</sup> C. D. Guzman,<sup>11</sup> D. Henry,<sup>2</sup> D. Holck,<sup>1</sup> Z. Hubert,<sup>3</sup> J. M. Huet,<sup>5</sup> A. Kellerer,<sup>12</sup> C. Kulcsar,<sup>13</sup> P. Laporte,<sup>5</sup> B. Le Roux,<sup>9</sup> N. Looker,<sup>1</sup> A. J. Longmore,<sup>2</sup> M. Marteau,<sup>3</sup> O. Martin,<sup>3</sup> S. Meimon,<sup>6</sup> C. Morel,<sup>3</sup> T. J. Morris,<sup>1</sup> R. M. Myers,<sup>1</sup> J. Osborn,<sup>1</sup> D. Perret,<sup>3</sup> C. Petit,<sup>6</sup> H. Raynaud,<sup>13</sup> A. P. Reeves,<sup>1</sup> G. Rousset,<sup>3</sup> F. Sanchez Lasheras,<sup>7</sup> M. Sanchez Rodriguez,<sup>7</sup> J. D. Santos,<sup>7</sup> A. Sevin,<sup>3</sup> G. Sivo,<sup>13</sup> E. Stadler,<sup>8</sup> B. Stobie,<sup>2</sup> G. Talbot,<sup>1</sup> S. Todd,<sup>2</sup> F. Vidal<sup>3</sup> and E. J. Younger<sup>1</sup>

<sup>1</sup>Department of Physics, Durham University, South Road, Durham DH1 3LE, UK

<sup>2</sup>UKATC, Royal Observatory, Blackford Hill, Edinburgh, EH9 3HJ, UK

<sup>3</sup>LESIA, Observatoire de Paris, CNRS, Univ. Paris Diderot, F-75014 Paris, France

<sup>4</sup>Issac Newton Group, Edificio Mayantigo, Calle Alvarez Abreu, 70, E-38700 Santa Cruz de la Palma, Canary Islands, Spain

<sup>5</sup>GEPI, Obs. de Paris, CNRS, Univ. Paris Diderot, F-92195 Paris, France

<sup>6</sup>ONERA, 29 Avenue de la Division Leclerc, F-92320 Chatillon, Paris, France

<sup>7</sup>Oviedo University, Calle San Francisco, 1, E-33003 Oviedo, Spain

<sup>8</sup>IPAG, Institut de Planetologie et d'Astrophysique de Grenoble, BP 53, F-38041 Grenoble, Cedex 9, France

<sup>9</sup>Laboratoire d'Astrophysique de Marseille, Rue Frederic Joliot Curie, F-13013 Marseille, France

<sup>10</sup>Herriot Watt University, Edinburgh Campus, Edinburgh EH14 4AS, UK

<sup>11</sup>Pontificia Universidad Católica de Chile, Avda Libertador Bernardo O'Higgins 340, 2354 5504 Santiago, Chile

<sup>12</sup>Cambridge University, Trinity Lane, Cambridge CB2 1TN, UK

<sup>13</sup>Institut d'Optique Graduate School, 2 Avenue Augustin Fresnel, F-91127 Palaiseau, Paris, France

Accepted 2016 March 24. Received 2016 March 23; in original form 2015 December 18

## ABSTRACT

Recent advances in adaptive optics (AO) have led to the implementation of wide field-of-view AO systems. A number of wide-field AO systems are also planned for the forthcoming Extremely Large Telescopes. Such systems have multiple wavefront sensors of different types, and usually multiple deformable mirrors (DMs). Here, we report on our experience integrating cameras and DMs with the real-time control systems of two wide-field AO systems. These are CANARY, which has been operating on-sky since 2010, and DRAGON, which is a laboratory AO real-time demonstrator instrument. We detail the issues and difficulties that arose, along with the solutions we developed. We also provide recommendations for consideration when developing future wide-field AO systems.

**Key words:** instrumentation: adaptive optics – instrumentation: detectors.

## 1 INTRODUCTION

The forthcoming Extremely Large Telescopes (ELTs; Johns 2008; Nelson & Sanders 2008; Spyromilio et al. 2008) all rely on adaptive optics (AO) systems (Babcock 1953) to provide atmospheric

\* E-mail: a.g.basden@durham.ac.uk

turbulence compensation and compensation for telescope vibrations due to wind loading and other motion. These AO systems are essential to allow scientific goals requiring high-resolution imaging and spectroscopy to be met. The vast majority of astronomical observations made with these telescopes will use wide field-of-view AO systems, including multi-conjugate AO, ground layer AO (GLAO), multi-object AO (MOAO) and laser tomographic AO (LTAO). These systems all use information from multiple wavefront sensors (WFSs) to provide a tomographic reconstruction of the Earth's atmospheric turbulence.

All current wide-field AO systems on existing telescopes have seen first light within the past decade, with facility class instruments such as GeMS (Rigaut et al. 2012) only undergoing commissioning in the past two years. Therefore, current operational experience is limited, and each system comes with its own complexities and problems.

The CANARY instrument (Myers et al. 2008; Gendron et al. 2011) on the William Herschel Telescope (WHT) is the most advanced wide-field AO test bed worldwide with an on-sky capability. It has been operated in MOAO, GLAO and LTAO modes, in addition to single-conjugate AO (SCAO) for comparative purposes. CANARY relies on both natural and laser guide stars, and has operated with both low- and high-resolution wavefront sensing modes. CANARY has been under continuous development having seen four major phases of operation, and with a sodium laser guide star (LGS) scheduled for commissioning in mid-2016. One outcome of this continuous development is that we have amassed extensive experience interfacing different WFS cameras with the CANARY real-time control system (RTCS), and have developed techniques to handle WFS synchronization in the presence of partial, corrupted or missing WFS frames, different WFS interfaces and unreliable camera interfaces. CANARY has also operated with several different deformable mirrors (DMs). In this paper, we discuss our experiences with WFS and DM interfaces to the CANARY RTCS.

The DRAGON AO test-bench at Durham University (Reeves et al. 2012) is a real-time wide-field AO demonstrator, which is used to explore wide-field AO techniques with high-order WFSs at 4–8 m telescope scales. This system models multiple natural guide stars (NGSs) and LGSs (including spot elongation and laser launch up-link through turbulence) and uses woofer–tweeter DM control (Hampton et al. 2006). Although the configuration of DRAGON is more permanent than that of CANARY (i.e. we will not be adding additional WFSs or DMs in the foreseeable future), it still provides us with experience with interfacing WFS cameras and DMs to the RTCS, and we discuss this experience here.

Both DRAGON and CANARY share a common RTCS, the Durham AO real-time controller (DARC), which is central processing unit (CPU) based with optional hardware acceleration facilities, including graphics processing units (GPUs) and field-programmable gate arrays (FPGAs; Basden et al. 2010). DARC is well suited for ELT-scale operation (Basden & Myers 2012). This common base allows WFS and DM interfaces to be shared between systems where necessary with little additional effort, and a CPU-based software on commodity hardware greatly simplifies the addition of new WFS camera and DM interfaces.

In Section 2, we provide a historical overview of the different CANARY operational phases, and of the WFS and DM interfaces developed. This gives a historical narrative of how the world-leading CANARY instrument was developed and built. We also provide this information for DRAGON. In Section 3, we discuss the challenges we experienced, and the techniques used to overcome these. We conclude in Section 4.

## 2 INTERFACES DEVELOPED FOR CANARY AND DRAGON

CANARY was first operated on-sky in 2010, with four NGSs, a single DM and a tip-tilt mirror, performing SCAO, MOAO and GLAO correction (phase A). During 2011, Rayleigh LGS commissioning was carried out, though without any AO correction (phase B0). In 2012, CANARY was operated with a single Rayleigh LGS and four NGSs (phase B1), and during 2013, was upgraded to include four LGSs (phase B2). In 2014, CANARY was reconfigured to operate in LTAO mode (phase C1), and in 2015, a second 241-actuator DM was added to create a split open/closed-loop system including woofer–tweeter operation (phase C2). Both the LGS and SCAO NGS WFSs were upgraded from  $7 \times 7$  to  $14 \times 14$  sub-apertures at this point. In 2016, a sodium LGS (launched far from the telescope axis, up to 40 m away) will replace the four Rayleigh LGSs, to allow investigation of extreme spot elongation and mitigation techniques (phase D). Additionally, CANARY will host a high-order SCAO upgrade, CHOUGH (Bharmal et al. 2014).

### 2.1 Phase A: interfacing four NGS and a DM

Initial designs for CANARY drew on experience gained by development of the European Southern Observatory SPARTA RTCS (Fedrigo et al. 2006), including the ability to use a modified SPARTA-Light wavefront processing unit (Suárez Valles et al. 2012) for computation of wavefront slopes in FPGA. The serial Front Panel Data Port (sFPDP) protocol was used for real-time communications. The CANARY RTCS is capable of operating on a pixel stream basis, rather than per-frame, i.e. processing commences as soon as the first pixels arrive at the RTCS, reducing the AO system latency. To use this capability, which is key to good AO performance, it is necessary to have access to the pixel stream produced by the camera, rather than (as with most commercial cameras) receiving access on a per-frame basis.

#### 2.1.1 WFS cameras

The CANARY design (Fig. 1) selected four Andor Technologies iXon 860 electron multiplying CCD (EMCCD) cameras, with a parallel Front Panel Data Port (pFPDP) output for the pixel stream, which was then converted to a fibre-based sFPDP protocol with pixels from pairs of cameras multiplexed together. This data stream (two sFPDP channels) was received using a commercial sFPDP Peripheral Component Interconnect (PCI) card in the RTCS server. The maximum frame rate achievable with these cameras was 300 Hz. Camera control (cooling, frame rate, triggering, etc.) was not via sFPDP; instead, the Andor Technologies software developer's kit (SDK) and PCI control card were used.

#### 2.1.2 Deformable mirror

The DM and tip-tilt mirror were controlled using a 96-channel PCI digital-to-analogue converter (DAC) card from United Electronic Industries, with custom electronics for voltage conversion. The DM itself was reused from the ADONIS AO system (Jagourel & Gaffard 1992), with 52 actuators ( $8 \times 8$ ) and recently characterized at LESIA (Kellerer et al. 2012). The tip-tilt mirror was made by Observatoire de Paris. A schematic diagram for phase A operation is given in Fig. 1

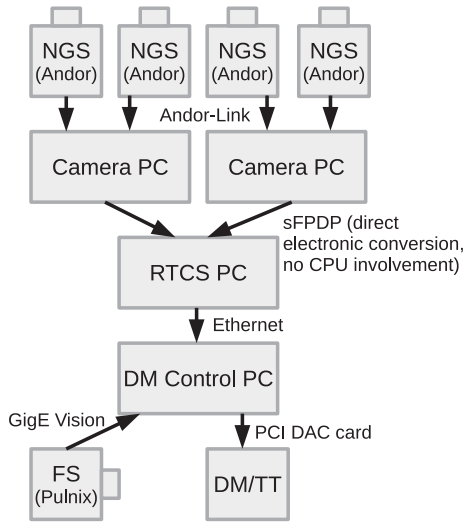


**Figure 1.** Phase A of CANARY showing the camera and DM connectivity. FS represents the figure sensor, TT is the tip-tilt mirror, PC represents a computer, NGS is a natural guide star wavefront sensor, RTCS is the real-time control system and DM represents deformable mirror.

### 2.1.3 Camera and DM control

A camera interface library module for DARC was developed to receive the sFPDP pixel streams. The DARC RTCS pipeline then de-multiplexed the pixel streams, calibrated the images, computed the wavefront slopes and performed wavefront reconstruction and DM fitting (using a single control matrix). Comprehensive lists of computational algorithms used in CANARY (and DRAGON) are given by Basden et al. (2010, 2014) and Basden & Myers (2012). The DM command vector was then output by sFPDP to a deformable mirror controller (DMC) server.

### 2.1.4 A figure sensor for open-loop DM control

The DM was operated in open loop, i.e. changes to the DM surface shape were not seen by the WFSs. The DMC included a figure sensor (a Shack–Hartmann WFS) that was used to monitor the shape of the DM, and then apply offsets to the DM command vectors so that the actual shape matched the requested shape as closely as possible. The figure sensor was to operate at a significantly higher frame rate than the NGS WFSs, so that the DM would move to its correct shape over the course of one NGS frame.

The figure sensor used a JAI Pulnix TM-6740GE camera, which had a GigE Vision interface (directly connected to the DMC), operating at up to 1 kHz frame rate for our region of interest. A DARC interface library was developed based on the camera manufacturer SDK.

### 2.1.5 Interface of the infrared science camera

A Xenics Xeva-1.7-320 camera was selected as a science point spread function measurement camera, with a maximum frame rate of 60 Hz. An interface module for this universal serial bus (USB) camera was created to allow operation with the RTCS, and it was operated with a separate instance of the RTCS on a dedicated science computer. Integrating this camera with the RTCS gave us several key abilities: the tools for operation of the camera and display and capture of information (locally and remotely) were identical to the rest of the system. Users therefore did not need to learn additional

interfaces. This camera was also used to provide tip-tilt closed-loop AO control during system calibration of the non-common path aberrations.

### 2.1.6 On-sky operation

For phase A of CANARY, we had two on-sky observing runs of four nights each. We were able to successfully demonstrate first MOAO operation, the capability of the Learn and Apply algorithm (Vidal et al. 2010), and first on-sky demonstration of GPUs for wavefront reconstruction.

## 2.2 Phase B0: LGS commissioning

Two pulsed 532 nm 20 W lasers were installed behind the WHT secondary mirror, to provide a single Rayleigh LGS using a polarization beam combiner. Further details are given by Morris et al. (2011). During operation, these lasers are pulsed at about 10 kHz, requiring a camera with a fast shutter to open and close once each pulse has propagated to and returned from the desired LGS height. Typically, this shutter will be open for 1  $\mu$ s per pulse with 100  $\mu$ s between pulses, ruling out any practical mechanical shutter. Therefore, a novel CCD architecture with an electronic (on-silicon) shutter (Lincoln Labs CCID18) was used with a Scimeasure controller and a custom sFPDP pixel stream interface. Unfortunately, this detector suffered electronic damage shortly before the on-sky commissioning, and so a temporary solution using Pockels cells and an Andor Technologies iXon camera was implemented whilst a replacement detector was sourced.

During LGS commissioning, a PCO.Edge scientific CMOS (sCMOS) camera was used to provide a wide-field image of the laser (unshuttered), and was interfaced with the DARC RTCS so that common software tools could be used, including pixel displays and camera controls, reducing duplication of effort. Pixel stream acquisition was not enabled for this camera: since it was not used in an AO loop, this was not required.

The two lasers were polarization combined to provide a single beam with increased power. A beam combining camera was installed to ensure that alignment of the lasers was maintained. This camera was an IDS Imaging UI-2210SE VGA camera, which was also integrated with the DARC RTCS. A separate instance of DARC was used for this camera, i.e. it was not associated with the main AO loop. The ability to automatically control the laser beam alignment was available because of the RTCS component. A closed-source SDK was used to create the DARC interface module.

### 2.2.1 On-sky operation

Phase B0 of CANARY received a total of three on-sky commissioning runs (a total of nine nights) in 2011–2012.

## 2.3 Phase B1: single LGS AO operation

After successful installation and testing of the lasers at the WHT, CANARY proceeded with the operation of a single LGS and four NGSs in 2012, as shown in Fig. 2. At this phase of CANARY, first successful on-sky demonstration of full linear–quadratic–Gaussian (LQG) SCAO operation was demonstrated (Sivo et al. 2014).

A custom infrared science camera using a NICMOS detector was introduced, replacing the previous science camera. This new detector had lower readout noise, and could operate with longer

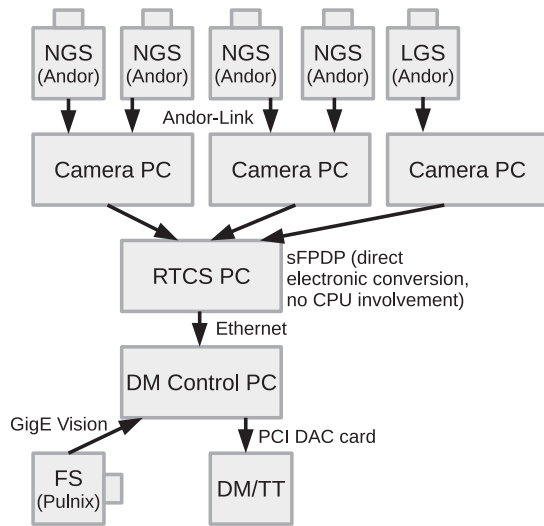


**Figure 2.** Phase B1 of CANARY showing the camera and DM connectivity. Here, LGS represents the laser guide star wavefront sensor.

exposure times. An interface module for the DARC RTCS was developed, based on a USB interface.

### 2.3.1 On-sky operation

Phase B1 of CANARY was operated with three on-sky observing runs (a total of 12 nights) in 2012.

## 2.4 Phase B2: operation with four LGSs

Four LGSs were imaged on to four quadrants of the repaired Scimeasure/CCID18 WFS camera, each with  $7 \times 7$  sub-apertures. A newer model of NGS WFS meant that maximum frame rate could now reach 450 Hz. A schematic diagram is shown in Fig. 3. At this phase of CANARY, on-sky demonstration of tomographic wavefront reconstruction using artificial neural networks was first demonstrated (Osborn et al. 2014), together with first demonstration of tomographic LQG control (Sivo et al. 2013).

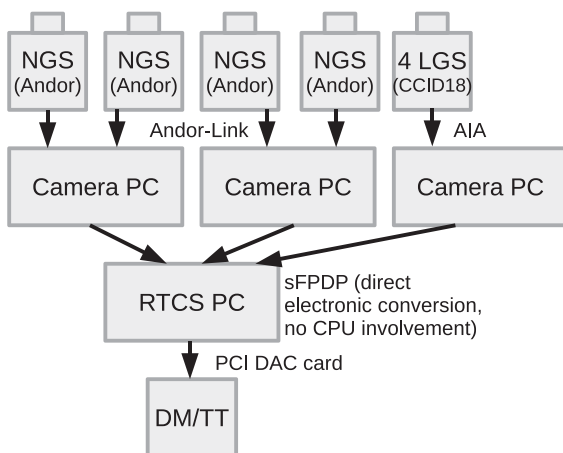


**Figure 3.** Phase B2 of CANARY showing the camera and DM connectivity.

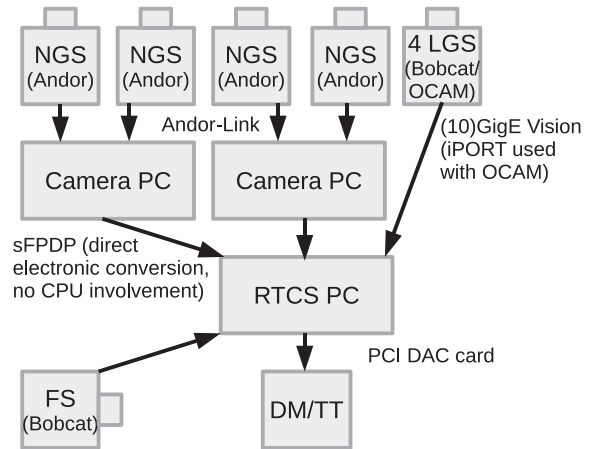


**Figure 4.** Phase C1 of CANARY showing the camera and DM connectivity.

### 2.4.1 On-sky operation

Two on-sky observing runs of six nights each were used for this phase of CANARY (B2) in 2013, following an initial three nights for LGS integration.

## 2.5 Phase C1: LTAO operation

CANARY was reconfigured into an LTAO system, by placing the DM in closed loop with the WFSs. At this stage, the LGS WFS camera had again failed, and a replacement was sought at short notice (1 month before on-sky operation). An Imperx Bobcat B0620 VGA camera was selected, using the interline transfer region as an electronic shutter. This camera had a GigE Vision interface. Read-out noise restricted LGS operation to about 12 km altitude (LGS return signal decreases rapidly with altitude). Mid-way through phase C1 (during the second set of on-sky nights), this LGS WFS was replaced by a First Light Imaging OCAM2S camera with developments specifically for CANARY (Gach et al. 2016), and a schematic diagram is shown in Fig. 4. The new camera allowed us to increase LGS altitude to about 20 km, though readout problems meant that the EMCCD gain mechanism was restricted.

At this phase, computation of pseudo-open-loop slopes became necessary. To aid this, a DM figure sensor was installed, this time using a Bobcat camera, operating as part of the main RTCS loop.

### 2.5.1 Integration of generic GigE Vision cameras

The necessity of pixel stream access meant that rather than using the closed-source Imperx SDK, we instead opted to use an open-source GigE Vision library (Aravis) with modification to provide low-latency pixel stream access, i.e. the ability to access User Datagram Protocol (UDP) packets (and thus begin data processing) as soon as they arrive, rather than waiting for the full frame.

The GigE Vision protocol is based on UDP packets, which are inherently unreliable: the Linux kernel can drop packets if processing load gets too high. Therefore, after investigation, it was determined that to operate these cameras reliably, a hard real-time kernel was necessary, and that the compute thread responsible for reading camera pixels must be restricted to run on CPU cores directly attached to the network card (by setting the thread affinity), with an elevated priority. After these steps are taken, UDP packet loss became negligible, with less than one packet loss per hour. The GigE Vision

interface module for the DARC system is suitable for operation with any GigE Vision camera.

### 2.5.2 Integration of the OCAM2S LGS WFS

Due to the urgent need to replace the Bobcat camera because of high readout noise, and to the very limited time available, a pragmatic approach was taken to integrate the OCAM2S camera. This camera has a Camera Link interface, and was (for the frame grabbers that we had available) restricted to full frame operation, i.e. pixel stream access was not possible. We therefore used a Camera Link to 10GigE Vision converter (an iPort CL-Ten from Pleora), and so could use our existing GigE Vision interface module for DARC. The additional latency introduced by the iPort was negligible, at the microsecond level, and the maximum CANARY frame rate remained restricted by the NGS WFS.

### 2.5.3 On-sky operation

Two on-sky observing runs (separated by about 3 months) of six nights each were used for this phase of CANARY (C1) in 2014.

## 2.6 Phase C2: Operation at increased WFS order and a woofer–tweeter configuration

In 2015, CANARY was upgraded to provide woofer–tweeter control (Hampton et al. 2006) and higher order LGS WFSs and SCAO WFS (the Truth sensor). To achieve this, an additional DM was added to the system (Fig. 5) in open loop (i.e. the WFSs were insensitive to changes of the DM surface), along with a corresponding figure sensor (a Bobcat). This tweeter DM was an ALPAO DM241, with  $17 \times 17$  actuators. The LGS WFS order was increased from  $7 \times 7$  sub-apertures to  $14 \times 14$ , again using the OCAM2S camera, this time with full functionality and sub-electron effective readout noise, allowing LGS height to be increased to about 30 km.

It should be noted that this configuration is deliberately similar to that proposed for the MOSAIC instrument (Evans et al. 2013) on the European ELT (E-ELT): a closed-loop DM (telescope M4) to provide GLAO correction and open-loop MOAO DMs. This demonstration was the original goal of CANARY, as proposed in 2007.

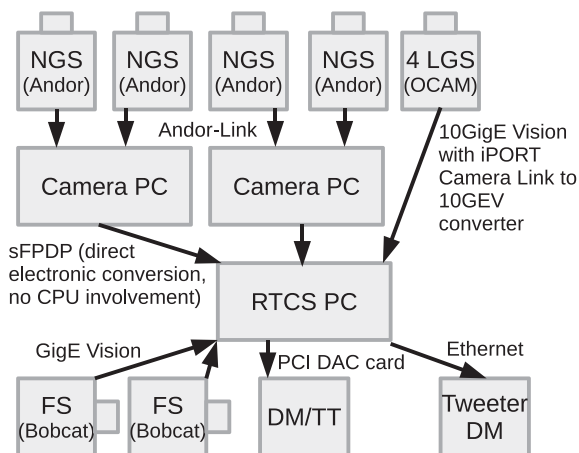


**Figure 5.** Phase C2 of CANARY showing the camera and DM connectivity.

### 2.6.1 Integration of the DM241

The new DM had an Ethernet interface and a closed-source binary SDK. Initial tests showed that there was some latency introduced by this interface, equal to about  $800 \mu\text{s}$  between DM demands being provided to the SDK and the mirror surface settling. For CANARY, the additional latency was not critical due to pseudo-open-loop operation, and we did not have time to develop an alternative solution.

To integrate the DM Ethernet interface with CANARY, a new interface module for DARC was developed, to allow operation of the woofer and tweeter together. The commissioning period of the upgraded system prior to on-sky operation was limited to about 1 month. However, due to the flexibility afforded by the DARC interface module system, integration of the new DM was straightforward and no problems arose.

### 2.6.2 On-sky operation

CANARY phase C2 operated with two on-sky observing runs of six nights each in 2015.

## 2.7 Phase D: extreme sodium LGS elongation

Phase D of CANARY is planned for the second half of 2016 (Rousset et al. 2014), and will replace the four Rayleigh LGS with a single sodium LGS, launched about 40 m from the telescope optical axis. During this phase, extreme spot elongation effects will be studied, with techniques developed to mitigate spot truncation and loss of sensitivity along the elongation axis. Designs for the E-ELT include sub-apertures that are about 40 m from the laser launch axis. Therefore, during CANARY phase D, we are treating the WHT as a sub-pupil of the E-ELT where LGS elongation is greatest. Two observing runs are planned, of six nights each.

During phase D, we will use the existing CANARY WFS cameras, each with  $7 \times 7$  sub-apertures. The LGS sub-apertures will have a field of view of 20 arcsec, to minimize spot truncation. We will also operate an LGS profiling camera on the nearby Isaac Newton Telescope, which will use a high-resolution sCMOS camera to image the LGS profile, allowing us to obtain high-resolution sodium layer profile images both to derive correlation and matched filter references and for further study of sodium layer variation. The existing sCMOS interface to the DARC RTCS will be used with modifications to allow dynamic resizing of the detector region of interest. A very simple three-mode active optics system will be implemented allowing control of tip, tilt and rotation (to keep the LGS elongation axis aligned with the detector pixels).

## 2.8 CANARY hosted high-order upgrade

The installation and test of a high-order AO instrument, CHOUGH (Bharmal et al. 2014), is also planned for 2016. This will see CANARY operating in SCAO mode with  $31 \times 31$  sub-apertures at a 1 kHz frame rate. The camera to be used at this stage is a Nüvü HNu 128  $\times$  128 EMCCD camera with a GigE Vision interface. The existing woofer–tweeter DMs will be used, along with a Boston Micromachines Kilo DM, described in Section 2.9.1.

## 2.9 The DRAGON wide-field AO bench

DRAGON aims to replicate CANARY concepts, to provide a single-channel MOAO system with a woofer–tweeter DM configuration, four NGSs and four LGSs each with  $30 \times 30$  sub-apertures. The

**Table 1.** A table summarizing key WFS parameters.

Model	Type	Phase	Information	Interface	Full source code
Andor iXon 860	NGS, LGS commissioning	A, B, C, D	EMCCD. PCI compatibility problems for sFPDP daughter board used to send pixel stream	Control via manufacturer PCI, pixels via sFPDP	Yes
Pulnix TM-6740GE	figure sensor	A	SDK unusable with modern Linux systems	GigE Vision	No
PCO.Edge 5.5	LGS commissioning	B0	sCMOS	Camera Link	No
UI-2210SE	LGS beam combination	B, C		USB-2	No
Xeva-1.7-320	IR science	A		USB-2	No
Camicaz	IR science	B, C, D	Custom built	USB-2	Yes
Scimeasure/CCID18	LGS	B2	Electronic silicon shutter	AIA to sFPDP	No
Bobcat B0620GE	LGS, figure sensor, NGS	C, D, DRAGON	C1 as LGS, NGS for DRAGON	GigE Vision	Yes
OCAM2S	LGS	C1, C2	Used with iPort converter	10GigE Vision	Yes
HS-2000	LGS	DRAGON		10GigE Vision	Yes
HNu 128	High-order SCAO	CHOUGH		GigE Vision	Yes

WFSs are all GigE Vision standard, with the NGS WFSs using the same model of Imperx Bobcat cameras as used by CANARY, and the LGS WFSs using an Emergent Vision Technologies HS2000 10GigE Vision camera. The DARC GigE Vision interface library is used with these cameras, and thus no new developments were required.

As a real-time research system, DRAGON enables verification of DARC developments using hardware acceleration including GPUs, and also many-core architectures such as the Xeon Phi (Barr et al. 2015) or POWER8 processors (Basden 2015). Currently, the DARC RTCS has the capability to use GPU acceleration, either just for wavefront reconstruction (first demonstrated on-sky in 2010 during CANARY phase A) or for the whole AO pipeline. Such hardware acceleration capabilities will provide the ability to service increased computational demands from future algorithm development.

### 2.9.1 DM integration

The woofer DM is a Xinetics 97-actuator DM controlled using a 96-channel PCI DAC card (United Electronic Industries, as used by CANARY) with the central actuator slaved to neighbours (since it is behind the central obscuration). The tweeter DM is a 1020-actuator Boston Micromachines Kilo DM ( $32 \times 32$  actuators) controlled using a PCIe fibre optic interface card provided by the DM manufacturer. The tip-tilt mirror is controlled using a 16-channel PCI DAC card (United Electronic Industries). A DARC interface library to control these DMs was required and developed.

## 2.10 Summary of WFS cameras used in CANARY and DRAGON

Table 1 provides a summary of key information about the WFS cameras that we have interfaced with DARC for operation with the CANARY and DRAGON wide-field AO systems.

## 3 CHALLENGES FOR WFS AND DM INTEGRATION

The integration of such a diverse set of cameras and DMs using a plethora of different interfaces meant that there were inevitable

challenges related to obtaining reliable operation, which we now discuss.

### 3.1 Missing camera data and dropped frames

For an AO system with multiple camera inputs, it should be assumed that at least occasionally, WFS data will fail to arrive at the RTCS: even in the case of perfect hardware, random events such as cosmic ray events could interfere. During CANARY phase A commissioning, we discovered that the NGS WFSs would regularly deliver partial frames, or insert an extra pixel into a frame. Initially, this occurred about once every 4 min. However, in later phases of CANARY, the frequency increased, and became less regular. Our understanding is that this is due to the implementation of the non-standard pFPDP interface, and is beyond our control. Therefore, a software fix, within the RTCS, was required.

When using UDP-based cameras (i.e. GigE Vision), packet loss is inevitable at some point, and so must be planned for.

#### 3.1.1 Software handling of incorrect camera data

Correct detection of incorrect camera data is key to AO performance. There are several cases that we have experienced, and thus consider within the DARC WFS interface modules.

(i) Dropped pixels: the data frame will be shorter than expected. This condition will be detected when the next start-of-frame signal arrives, after pipeline computation from all other WFSs has completed.

(ii) Inserted pixels (e.g. a single pixel being duplicated and thus received twice): the end-of-frame signal will be incorrect. This condition will be detected at the end of the frame, probably after pipeline computation has completed, i.e. wavefront reconstruction will have been performed based on corrupt data.

(iii) Complete frame missing: the DARC interface will not receive any data for this frame. This condition will be detected when AO pipeline computation for all other WFS interfaces has completed and not yet started for the dropped frame.

(iv) Dropped Ethernet packets: UDP packets from GigE Vision cameras fail to arrive. This condition is detected using the packet counter embedded within packets, and will be detected as soon as the



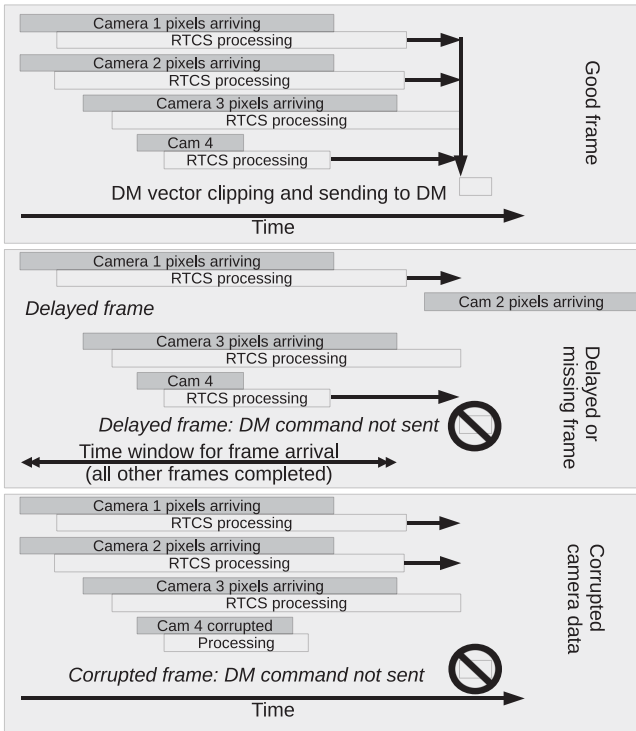


**Figure 6.** A figure showing three cases for pixel arrival. The top portion shows a good frame with all pixels arriving as expected. The middle case shows the action taken if one camera is delayed to beyond all others being finished (or fails to arrive). The third case shows arrival of a corrupted frame.

next packet arrives, while pipeline computation is ongoing. Within our interface, we do not make allowance for packet reordering since we have not discovered this occurring. Therefore, an out-of-order packet is taken to signify a missing packet.

These error conditions are detected and handled by DARC. Upon detection, a flag is set to specify that the DM command vector should be frozen for that frame, and that the integrator should not be accumulated. Fig. 6 demonstrates a time-line for three cases. During a good frame, the pixels from different camera types arrive and are processed. Note that different arrival times are due to the differences in camera readout times (different camera models). In the second case, the arrival of a camera frame is delayed until after all other cameras have finished readout, this is detected and the pipeline aborted, i.e. DM commands are not sent. In the third case, a corrupted frame is detected in one camera, processing is aborted and DM commands are not sent.

Internally in DARC, one CPU thread is dedicated to each camera to transfer pixels into a circular buffer for further processing by the CPU threads responsible for RTCS pipeline computation, which we term sub-aperture processing threads. Processing of these pixels proceeds as soon as enough pixels to fill a given sub-aperture have arrived, and a single thread then calibrates the sub-aperture, computes the wavefront slope and performs a partial wavefront reconstruction. We term this a horizontal processing strategy, and further information is given by Basden et al. (2010). The pixel arrival buffers are typically quadruple buffered, i.e. a circular buffer with space for four camera frames, though this depends on the DARC camera module being used. Fig. 7 provides a schematic diagram of this approach. Quadruple buffering will ensure that with a real-time kernel no data are overwritten before it has been processed, and that with a non-real-time kernel, this is also very unlikely.

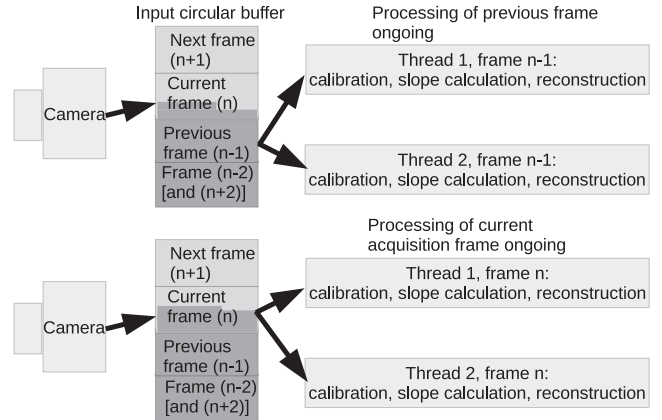


**Figure 7.** A figure showing how pixel data are handled in DARC. Camera pixels are directed to a small circular buffer which is then read by the sub-aperture processing threads. In the upper half, these threads are processing a completed frame, and in the lower half, the threads have moved on to begin processing the next, currently incomplete, frame.

Due to the use of this horizontal processing strategy, the detection and mitigation of corrupted image frames is non-trivial: by the time an error condition is detected, most of the computation for this and other WFSs will already have been performed, including wavefront reconstruction, update (decay) of the integrator and update of sub-aperture tracking algorithms (adaptive windowing). It is therefore necessary to reset these parameters to the previous state. It is absolutely essential to ensure that DM command vectors are *never* sent to the DM based on a corrupted camera frame. Temporal forecasting from a previous frame is not a necessary strategy for CANARY-scale systems: simply freezing the DM state for a frame does not significantly degrade performance (Section 3.1.2).

Maintaining synchronization between the different WFSs (i.e. so that one camera does not lag others by an integer number of frames) is achieved by only using the most recent whole or partial frame after a previous frame has finished. As previously mentioned, one CPU thread per camera is used to transfer pixels into a circular buffer. When starting a new frame, the sub-aperture processing threads first check whether there is currently an active frame being read from the camera (i.e. whether the first pixels have already arrived). In this case, this frame then proceeds to be processed. If this is not the case (i.e. there is not currently a frame arriving), then the most recently acquired frame will be processed if it has not already been processed. In this way, if a WFS does begin to lag (if, for example, another WFS has missed a frame), a frame will be dropped, and differential latency removed. Although this approach might seem obvious, it is worth a mention here as an issue that requires thought, i.e. is non-trivial. We note that this approach enables reliable operation on non-real-time operating systems, i.e. scheduling delays do not allow frames to stack up for processing.

### 3.1.2 Impact of corrupt image frames

The effect of missing or corrupt image frames on AO performance for CANARY is relatively low. Being a moderate-order (pseudo-) open-loop AO system, AO bandwidth error forms a relatively small part of the overall error budget, and so the occasional additional single frame of latency has little impact. Fig. 8 shows Monte Carlo simulation results (*H*-band rms wavefront error) for a CANARY-like system (using only the on-axis Truth sensor) as a function of probability of missing WFS frames. These results are for a SCAO

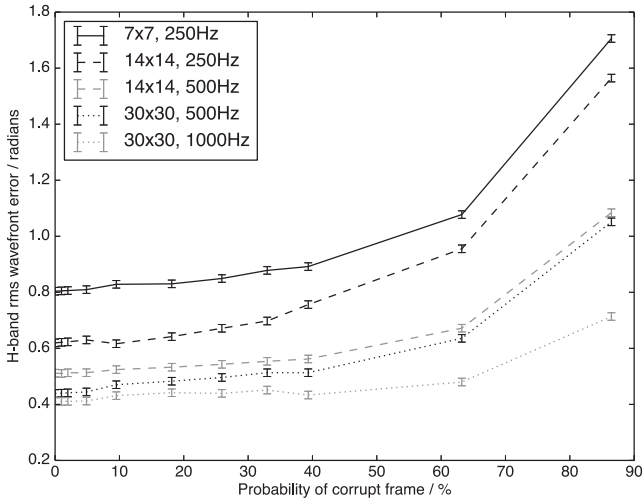


**Figure 8.** A figure showing AO performance (rms residual wavefront error) as a function of probability of a corrupt WFS frame (for any given frame). For CANARY, this probability is well below 1 per cent.

system on a 4.2 m telescope and consider a  $7 \times 7$ ,  $14 \times 14$  and  $30 \times 30$  order AO system (Fried geometry), relevant for the different phases of CANARY, and for CHOUGH and DRAGON, at different frame rates. It can be seen that when the probability of a missing frame is low (1 per cent), the impact on performance is negligible. For the CANARY WFSs, the probability of a corrupt frame was found to be below the 0.1 per cent level, and therefore we are confident that our occasional corrupt frame has not reduced AO performance with any significance: other errors dominate. Nevertheless, we recommend that WFS cameras should be well tested for these transient errors before acceptance.

These Monte Carlo simulations use parameters that are used during CANARY design studies, including a three-layer atmosphere with a Fried’s parameter of 12 cm and an outer scale of 30 m. Within the simulation, a corrupt image frame would be simulated with a specified probability (Poisson distributed), which would then result in the DM being frozen for that frame.

Our technique for freezing system state within DARC (e.g. resetting integrators to their previous values) upon detection of a corrupt frame also applies to pseudo-open-loop slope calculation.

### 3.2 Camera trigger synchronization

Cameras in both CANARY and DRAGON are externally triggered using a common frequency trigger signal, though with a selectable delay for each camera. For most phases of CANARY, this delay was set so that the last pixel of each frame from each camera would arrive at the RTCS at the same time. This approach minimized latency, allowing the DM shape to be set as soon as possible relative to the camera exposures. However, this approach means that different cameras are exposed for different periods of time, leading to complications for pseudo-open-loop control operation during phase C. At this point, we therefore triggered cameras to have the same mid-point exposure time (i.e. the middle of the exposure coincided for all cameras).

Camera synchronization can also be complicated by the inclusion of integrated electronic shutters that are used with the Rayleigh LGS WFS detectors. Whilst this is by no means a standard technology used within astronomy, the development of pulsed sodium lasers may mean that it becomes a standard requirement. Dependent on

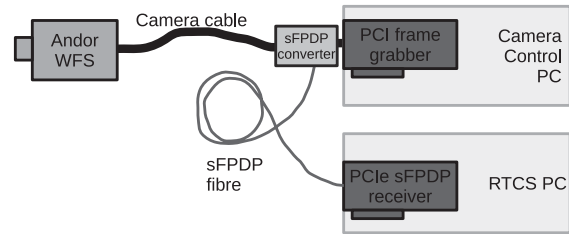


**Figure 9.** A figure showing hardware used to access the pixel stream from Andor iXon cameras.

the implementation of the shuttering within the camera, the laser pulses must also be synchronized to the camera readouts, requiring a centralized timing system capable of nanosecond jitter feeding signals to several distributed locations across the telescope.

### 3.3 Camera driver issues

Over the operational period of CANARY, we have had a large number of different cameras interfaced to the CANARY RTCS system. Most of these cameras have relied on closed-source software drivers, and as a result we have experienced incompatibilities between required Linux kernel specifications and software stacks, particularly for older cameras which often do not see the related software updated for newer Linux kernels.

For operation at phase A, we obtained (under a non-disclosure agreement) source code for the sFPDP receiver card used for capture of NGS pixels. This was then essential at phase C when we upgraded the RTCS server, to allow the sFPDP interface to continue to work with a newer Linux kernel. EMCCD camera control was performed using the standard camera interface card from Andor Technologies, which has good driver support. Unfortunately, our extension to enable a sFPDP pixel stream relies on a PCI card that we have only managed to operate with one specific motherboard type, and of which our spare supplies are running low. We have therefore developed a new method for producing the sFPDP stream, using an FPGA-based board which attaches to the standard Andor Technologies camera output, acting as a pass-through device for the standard image data, and also providing a sFPDP (or Ethernet) pixel stream, as shown in Fig. 9. This system is likely to be used from 2016 onwards.

The Pulnix camera used a binary SDK last updated in 2009, to which source code access was not available. Fortunately, this camera was only required for phase A, and so future compatibility has not been an issue. Should we require use of this camera in the future, the newer generic GigE Vision DARC interface (for which full source code is available) would be used, also having the advantage of pixel stream access.

The sCMOS camera has a Camera Link interface, and requires closed-source drivers for the frame grabber, as well as for the camera SDK (from different manufacturers). As of 2015, these drivers have remained in active development, and it has been possible to continue to operate the camera with up-to-date Linux kernels. However, obtaining these drivers can be difficult.

The Scimeasure controller for the CCID18 detector uses an AIA frame grabber card (necessary for camera control, even though we use sFPDP for receiving the pixel stream), requiring a PCI interface (which are becoming less common). Drivers are still available, though in binary format from the frame grabber manufacturer. A waveform compiler is also necessary, and exists as a Windows executable (which we use on Linux under Wine).

As mentioned previously, our discovery of the open-source Aravis library for GigE Vision cameras and our modification of it meant that any GigE Vision camera now has an interface to DARC which relies only on the presence of a network interface, rather than a commercial frame grabber. In the case of the OCAM2S camera, a close collaboration with the camera manufacturer, and an investigation of UDP packets, was necessary to develop a functional solution including full camera control.

### 3.4 Cabling of cameras

The stability of an AO bench is paramount and it is necessary to keep electronic and computer racks some distance from the optics to avoid heating, air-flow and vibration effects. For CANARY, where possible, computers and electronics are located in an electronics room, adjacent to the optical bench area.

The available cable length for our Andor Technologies cameras was limited such that we had the controller PCs mounted on an above-bench frame, with the sFPDP link extending from these PCs to the RTCS (with fibre length being essentially unlimited for our purposes).

For Ethernet-based cameras, cable length is not an issue, as Ethernet cable lengths are ample for our requirements. Camera Link cables of up to 10 m lengths are also available, again allowing a direct connection between camera and the RTCS in a separate electronics room. We have found that some Ethernet cameras get hot during operation, which means thermal control should also be considered.

### 3.5 DM driver issues

The low-order CANARY and DRAGON DM and tip-tilt mirrors are controlled using custom electronics driven from a commercial PCI DAC card. We have access to the source code for the drivers of this card, which has allowed us to make modifications for newer Linux kernels.

The high-order CANARY DM is operated using Ethernet, though this solution still required use of a closed-source binary (at the user level, i.e. without any kernel drivers necessary).

The Boston Kilo DM uses a PCIe fibre card, for which closed-source drivers are available for Linux. Fortunately, the Kilo DM drive electronics are modular, allowing a different DM interface to be used in the future, should the need arise.

### 3.6 Lessons learnt and key points for consideration

Our extensive experience with WFSs and DMs for wide-field AO systems has provided us with several key considerations to be taken into account during the design of future AO systems. Many of the problems that we encountered were specific to CANARY; however, the lessons that we learned are highly relevant for future AO systems. Closed-source drivers and binary SDKs are problematic because of potential future incompatibilities with newer Linux kernels due to changes in the application binary interface specification, and should be avoided where possible. Systems using commonly available hardware interfaces such as Ethernet should be favoured, and pixel stream access will significantly reduce AO latency. Maximum cable lengths should also be given consideration. As astronomical AO technology becomes more mainstream, emphasis on commodity hardware and open-source software becomes increasingly important.

Synchronization of WFSs and correct handling of corrupted image frames is non-trivial due to the pipeline nature of AO processing, and should be considered at the design phase of AO system development. The impact of corrupted frames on all aspects of the system (telescope offloads, telemetry data storage, etc.) should be considered.

A single RTCS system with which to operate all cameras has also been beneficial (including cameras that are not WFSs), allowing a single interface to be used, significantly reducing the learning curve for system developers. This also reduces the effort required to develop camera control tools, graphical interfaces, etc., and simplifies project development.

## 4 CONCLUSIONS

The CANARY AO demonstrator instrument has been operated on-sky over a 6-yr period, with many different instrument development phases, aimed at testing and demonstrating new AO concepts and technologies. During this period, we have acquired significant expertise related to integration of WFS cameras and DMs with the AO RTCS, DARC. Here, we have described the different phases of CANARY operation, providing details of the WFS and DM interfaces required at each phase, and how these have been integrated with the system. An overview of the DRAGON AO bench has also been given, along with the approach taken for integration of WFSs and DMs with the RTCS. We have discussed the problems that were met and overcome, and have provided recommendations for future AO systems. In summary, for long-life expectancy AO systems, we recommend the use of Ethernet-based cameras and DMs where possible to extend operational instrument lifetime, to enable continued compatibility during future system updates, and to remove the requirement for product-specific frame grabbers or other hardware. Open-source software or, as a minimum, access to source code for all kernel module driver interfaces greatly increases the future maintainability of these systems, allowing continued developments, updates and repairs to be made.

## ACKNOWLEDGEMENTS

This work is funded by the UK Science and Technology Facilities Council, grant ST/K003569/1, and a consolidated grant ST/L00075X/1. DG appreciates support from FONDECYT grant 1150369. Supported in France by Agence Nationale de la Recherche (ANR) programme 06-BLAN-0191, CNRS/INSU, Obs. de Paris and Univ. Paris Diderot; supported by European Commission FP7: E-ELT Prep. Infrastruct. 2007-1 Grant 211257, OPTICON programme Infrastructures 2008-1 Grant 226604 (JRA1) and 2012-1 Grant 312430 (WP1).

## REFERENCES

- Babcock H. W., 1953, PASP, 65, 229
- Barr D., Basden A. G., Dipper N., Schwartz N., 2015, MNRAS, 453, 3222
- Basden A. G., 2015, MNRAS, 432, 1694
- Basden A. G., Myers R. M., 2012, MNRAS, 424, 1483
- Basden A. G., Geng D., Myers R., Younger E., 2010, Appl. Opt., 49, 6354
- Basden A. G., Bharmal N. A., Bitenc U., Dipper N., Morris T., Myers R., Reeves A., Younger E., 2014, in Proc. SPIE Conf. Ser. Vol. 9148, Adaptive Optics Systems IV. SPIE, Bellingham, p. 91484F
- Bharmal N. A., Myers R. M., Basden A. G., Hölck D., Morris T. J., 2014, in Marchetti E., Close L., Veran J.-P., eds, Proc. SPIE Conf. Ser. Vol. 9148, Adaptive Optics Systems IV. SPIE, Bellingham, p. 91485V
- Evans C. et al., 2013, preprint ([arXiv:1303.0029](https://arxiv.org/abs/1303.0029))

- Fedrico E., Donaldson R., Soenke C., Myers R., Goodsell S., Geng D., Saunter C., Dipper N., 2006, in Ellerbroek B. L., Bonaccini Calia D., eds, Proc. SPIE Conf. Ser. Vol. 6272, *Advances in Adaptive Optics II*. SPIE, Bellingham, p. 627210
- Gach J.-L. et al., 2016, in Gavel D., Trancho G., eds, Proc. 4th AO4ELT Conference, OCAM2S: An Integral Shutter Ultrafast and Low Noise Wavefront Sensor Camera for Laser Guide Stars Adaptive Optics Systems. Centre of Adaptive Optics, Univ. California, p. 58
- Gendron E., Vidal F., Brangier M., Morris T., Hubert Z., Basden A. G., Rousset G., Myers R., 2011, *A&A*, 529, L2
- Hampton P., Bradley C., Agathoklis P., Conan R., 2006, in Ryan S., ed., *The Advanced Maui Optical and Space Surveillance Technologies Conference. Control System Performance of a Woofer-Tweeter Adaptive Optics System*. The Maui Economic Development Board, Hawaii, p. 59
- Jagourel P., Gaffard J.-P., 1992, in Ealey M. A., ed., Proc. SPIE Conf. Ser. Vol. 1543, *Active and Adaptive Optical Components*. SPIE, Bellingham, p. 76
- Johns M., 2008, in Andersen T., ed., Proc. SPIE, Vol. 6986, *Extremely Large Telescopes: Which Wavelengths? Retirement Symposium for Arne Ardeberg*. SPIE, Bellingham, p. 698603
- Kellerer A., Vidal F., Gendron E., Hubert Z., Perret D., Rousset G., 2012, in Ellerbroek B., Marchetti E., Veran J.-P., eds, Proc. SPIE Conf. Ser. Vol. 8447, *Adaptive Optics Systems III*. SPIE, Bellingham, p. 844765
- Morris T., Hubert Z., Chemla F., Todd S., Gendron E., Huet J.-M., Younger E., Basden A. G., 2011, in *Second International Conference on Adaptive Optics for Extremely Large Telescopes*. Available at <http://ao4elt2.lesia.obspm.fr>
- Myers R. M. et al., 2008, in Hubin N., Max C. E., Wizinowich P. L., eds, Proc. SPIE Confer. Ser. Vol. 7015, *Adaptive Optics Systems*. SPIE, Bellingham, p. 70150E
- Nelson J., Sanders G. H., 2008, in Stepp L., Gimozzi R., eds, Proc. SPIE Conf. Ser. Vol. 7012, *Ground-based and Airborne Telescopes II*. SPIE, Bellingham, p. 70121A
- Osborn J. et al., 2014, *MNRAS*, 441, 2508
- Reeves A. P. et al., 2012, in Ellerbroek B., Marchetti E., Veran J.-P., eds, Proc. SPIE Conf. Ser. Vol. 8447, *Adaptive Optics Systems III*. SPIE, Bellingham, p. 84474Y
- Rigaut F. et al., 2012, in Ellerbroek B., Marchetti E., Veran J.-P., eds, Proc. SPIE Conf. Ser. Vol. 8447, *Adaptive Optics Systems III*. SPIE, Bellingham, p. 84470I
- Rousset G. et al., 2014, in Marchetti E., Close L., Veran J.-P., eds, Proc. SPIE Conf. Ser. Vol. 9148, *Adaptive Optics Systems IV*. SPIE, Bellingham, p. 91483M
- Sivo G. et al., 2013, in Esposito S., Fini L., eds, Proc. 3rd AO4ELT Conference, *First On-sky Validation of Full LQG Control with Vibration Mitigation on the CANARY MOAO Pathfinder*. INAF - Osservatorio Astronomico di Arcetri, Italy, p. 127
- Sivo G., Kulcsar C., Conan J., Raynaud H., Gendron E., Basden A. G., Vidal F., Morris T., 2014, *Opt. Express*, 22, 23565
- Spyromilio J., Comerón F., D’Odorico S., Kissler-Patig M., Gilmozzi R., 2008, *The Messenger*, 133, 2
- Suárez Valles M., Fedrico E., Donaldson R. H., Soenke C., Zampieri S., Bourtembourg R., Tischer H., 2012, in Ellerbroek B., Marchetti E., Veran J.-P., eds, Proc. SPIE Conf. Ser. Vol. 8447, *Adaptive Optics Systems III*. SPIE, Bellingham, p. 84472Q
- Vidal F., Gendron E., Brangier M., Sevin A., Rousset G., Hubert Z., 2010, in Clenet Y., Conan J.-M., Fusco T., Rousset G., eds, *Adaptive Optics for Extremely Large Telescopes*. EDP Sciences, France

This paper has been typeset from a  $\text{\TeX}/\text{\LaTeX}$  file prepared by the author.